Am J Physiol Renal Physiol 299: F1339–F1347, 2010.
First published September 1, 2010; doi:10.1152/ajprenal.00077.2010.

The transcription factor HNF1α regulates expression of chloride-proton exchanger ClC-5 in the renal proximal tubule

Karo Tanaka,[1]* Sara Terryn,[2]* Lars Geffers,[3] Serge Garbay,[4] Marco Pontoglio,[4] and Olivier Devuyst[2]

[1]*Department of Pharmacology, Teikyo University School of Medicine, Tokyo, Japan;* [2]*Nephrology Unit, Université Catholique de Louvain Medical School, Brussels, Belgium;* [3]*Department of Genes and Behavior, Max-Planck-Institute for Biophysical Chemistry, Göttingen, Germany; and* [4]*INSERM U567, CNRS UMR 8104, Université Paris-Descartes, Team 26, Institut Cochin, Paris, France*

Submitted 8 February 2010; accepted in final form 30 August 2010

Tanaka K, Terryn S, Geffers L, Garbay S, Pontoglio M, Devuyst O. The transcription factor HNF1α regulates expression of chloride-proton exchanger ClC-5 in the renal proximal tubule. *Am J Physiol Renal Physiol* 299: F1339–F1347, 2010. First published September 1, 2010; doi:10.1152/ajprenal.00077.2010.—The Cl^-/H^+ exchanger ClC-5 is essential for the endocytic activity of the proximal tubule cells and the tubular clearance of proteins filtered in the glomeruli. The mechanisms that regulate the expression of ClC-5 in general and its specific expression in the proximal tubule are unknown. In this study, we investigated the hypothesis that the hepatocyte nuclear transcription factor HNF1α, which is predominantly expressed in proximal tubule segments, may directly regulate the expression of ClC-5. In situ hybridization demonstrated that the expression of *Clcn5* overlaps with that of *Hnf1α* in the developing kidney as well as in absorptive epithelia, including the digestive tract and yolk sac. Multiple binding sites for HNF1 were mapped in the 5′-regulatory sequences of the mouse and human *Clcn5/CLCN5* genes. The transactivation of the *Clcn5/CLCN5* promoter by HNF1α was verified in vitro, and the binding of HNF1α to the *Clcn5* promoter in vivo was confirmed by chromatin immunoprecipitation in mouse kidney. The expression of *Clcn5* was reduced in the proximal tubule segments of HNF1α-null kidneys, and it was rescued upon transfection of HNF1α-null cells with wild-type but not with mutant HNF1α. These data demonstrate that HNF1α directly regulates the expression of ClC-5 in the renal proximal tubule and yield insights into the mechanisms governing epithelial differentiation and specialized transport activities in the kidney.

endocytosis; Dent's disease; absorptive epithelia

CHLORIDE TRANSPORTERS EXPRESSED in renal epithelial cells are involved in a range of physiological processes, including regulation of cell volume or intracellular pH, acidification of intracellular vesicles, and transepithelial transport (8). These functions rely on the specific distribution and regulation of the various transporters in distinct tubular segments. The cells lining the proximal tubule (PT) are characterized by an intense endocytic activity, responsible for the tubular clearance of most proteins filtered in the glomeruli (5). Chloride ions have long been considered important for endocytosis, because the influx of negative charges partially neutralizes the transmembrane potential generated by the vacuolar proton ATPase (V-ATPase), thus facilitating vesicular acidification and progression along the endocytic apparatus (23). The characterization of two independent knockout (KO) mice has shown that the endosomal Cl^-/H^+ exchanger ClC-5 is essential for the endocytosis mediated by PT cells (28, 43).

ClC-5 is a member of the CLC family of Cl^- channels and Cl^-/H^+ exchangers that is primarily expressed in renal PT endosomes (7, 12). Heterologous expression studies have shown that ClC-5 operates as an electrogenic Cl^-/H^+ exchanger (35) that facilitates the acidification of PT endosomes (13). Defective endocytosis underlines the low-molecular-weight proteinuria and PT dysfunction in patients with Dent's disease (20, 36) and in ClC-5 KO mice (28, 43). In addition to its predominant expression in PT cells, ClC-5 is also expressed in the cells lining the thick ascending limb (TAL) and collecting duct (CD) nephron segments (7, 12) and in the epithelial cells lining the small intestine and colon of rats, which have morphological and functional similarity (e.g., high absorptive and endocytic activity) with PT cells (42). The mechanisms involved in the regulation of ClC-5 expression and its specific distribution in reabsorptive epithelia and PT segments in particular remain unknown.

The homeodomain-containing hepatocyte nuclear factor 1α (HNF1α) is expressed in specialized epithelial cells of the liver, kidney, intestine, and pancreas, which are actively involved in absorption and secretion processes (41). In particular, HNF1α regulates the transcription of major plasma proteins as well as products synergistically involved in carbohydrate metabolism, bile acid and cholesterol metabolism (29, 37, 40). Heterozygous mutations in HNF1α are a common cause of an autosomal dominant form of diabetes mellitus characterized by early age of onset and pancreatic β-cell dysfunction (maturity-onset diabetes of the young type 3; MODY3) (9). In the mouse kidney, HNF1α is predominantly expressed in PT segments, and its inactivation, which does not affect nephrogenesis, is reflected by a defective reabsorption of glucose and phosphate due to a reduced expression of the Na^+/glucose cotransporter SGLT2 (SLC5A2) and the Na^+/phosphate cotransporter NPT1 (SLC17A1), respectively (4, 29, 31). A closely related transcription factor named HNF1β, which is expressed earlier during development and detected in all nephron segments except the glomerulus, has also been characterized (18, 29). Based on the expression of HNF1α in PT segments and the fact that its inactivation is reflected by downregulation of plasma membrane transporters active in PT cells, we hypothesized that HNF1α may be involved in the segment-specific regulation of ClC-5. To investigate this possibility, we determined the tissue-specific expression patterns of *Clcn5* and *Hnf1α* during mouse development and nephrogenesis. We examined the 5′-regulatory sequences of mouse *Clcn5* and human *CLCN5* for HNF1 binding sites and used chromatin immunoprecipita-

* K. Tanaka and S. Terryn contributed equally to this study.

Address for reprint requests and other correspondence: O. Devuyst, Div. of Nephrology, UCL Medical School, 10 Ave. Hippocrate, B-1200 Brussels, Belgium (e-mail: olivier.devuyst@uclouvain.be).

tion (ChIP) to confirm the in vivo binding of HNF1α to the *Clcn5* promoter. The transactivation of the *Clcn5/CLCN5* promoter by HNF1α was verified in vitro and in PT segments and cells from *Hnf1α*-null mice. Taken together, our data demonstrate that HNF1α directly regulates the expression of the endosomal Cl^-/H^+ exchanger ClC-5 in the PT of the kidney.

MATERIALS AND METHODS

In situ hybridization in mouse embryos. Whole mount in situ hybridization was carried out using standard procedures (33). Briefly, mouse embryos were dissected between *day 9.5* (*E9.5*) and *E12.5* of gestation, fixed in 4% paraformaldehyde, treated with proteinase K, refixed, and hybridized overnight at 68°C with a digoxigenin-labeled antisense riboprobe transcribed in vitro from a 1.6-kb cDNA fragment of the 3′-end of the *Clcn5* open reading frame. High-stringency washing at 68°C was used, followed by incubation with anti-digoxigenin-AP antibody (Roche Applied Science, Mannheim, Germany) and revelation with nitroblue tetrazolium chloride and 5-bromo-4-chloro-3-indolylphosphate. Control hybridization was performed with a sense probe derived from the same cDNA template.

In situ hybridization studies for localization of *Hnf1α*, *Clcn5*, and *MyoD* in mouse *E14.5* embryos were performed as described earlier (26). Gene expression was detected using digoxigenin-labeled antisense riboprobes generated by in vitro transcription from DNA templates which were PCR-amplified from mouse *E14.5* cDNA. Images and associated metadata were deposited in a public database (http://www.genepaint.org).

In silico identification of putative HNF1 binding sites. DNA sequence information is based on the mouse and human genome assemblies NCBI37/mm9 and NCBI36/hg18, respectively. The search for putative HNF1 binding sites at the gene loci of ClC-5 and other members of the CLC gene family was performed as previously described (40), and results were displayed using the University of California Santa Cruz Genome Browser. A matrix comparison of the 5′ sequence of *CLCN5/Clcn5* genes was used to generate a dot plot that identifies regions of similarity between the two sequences (21).

Nuclear extracts and bandshift assay. Nuclear extracts from freshly dissected rat liver were prepared as described (10), with all buffers containing protease inhibitors aprotinin (1 μg/ml), benzamidine (2 mM), and PMSF (0.5 mM). Sense and antisense oligonucleotides for putative HNF1 binding sites, mBS-1 (+1931) and hBS-3 (−1056), were synthesized, and the forward strands were end-labeled with γ-[^{32}P]ATP by T4 polynucleotide kinase. Double-stranded probes (1 ng) were incubated with 5 μg of the nuclear extracts for 10 min in a final volume of 14 μl. Samples were then subjected to electrophoresis on a 6% polyacrylamide gel and autoradiography. For competition assays, a 50-fold molar excess of unlabeled oligonucleotides was added to the reaction mixtures.

Chromatin immunoprecipitation assay. Chromatin immunoprecipitation (ChIP) was performed as described previously (11). Nuclei were prepared from pooled kidneys of C57BL/6 mice, and primers were designed using PrimerExpress 2.0 software (Supplemental Table 1; supplementary material for this article is available online on the Journal web site). Quantification of immunoprecipitated DNA fragments was carried out in triplicate on an ABI PRISM 7000 system using SYBR green fluorescent dye (Applied Biosystems, Foster City, CA). The relative DNA enrichment was based on the formula ($ChIP_{target}$/$ChIP_{normalizer}$)/($imput_{target}$/$imput_{normalizer}$). A DNA fragment in the first intron of aortic smooth muscle α-actin 2 gene (*Acta2*), which lacks any HNF1 binding site, was used as a negative control. Specificity of the HNF1α antibody was previously established (6, 11).

Isolation and subcloning of CLCN5-regulatory sequences. The luciferase vectors containing mouse *Clcn5* 5′-regulatory sequences were previously constructed (38). The human X chromosome-specific cosmid library ICRF104 (L4/FSC X) was screened using a cDNA fragment of the 5′-end of *CLCN5*, and the 5-kb *Bam*HI/*Xho*I genomic fragment containing ~2.5 kb upstream of the transcription start site to exon 2 was subcloned into the pXP2 promoterless luciferase vector.

Cell culture, transient transfection, and luciferase reporter assay. Monkey kidney COS-7 cells and human epithelial cervical carcinoma C33 cells were cultured in DMEM containing 10% FCS, and the reporter gene assay was performed as previously described (38). Briefly, the constructs were transiently transfected by the calcium phosphate method at a vector DNA dose of 500 ng per 1×10^5 cells, and their luciferase activities were measured compared with that of empty vector pXP2. An expression vector pRSV-β-galactosidase was used for the normalization of transfection efficiency. For the coexpression analysis, an expression vector pRSV-HNF1α was included in the transfection at a dose of 500 ng per 1×10^5 cells. The total DNA content per transfection was equalized with pGEM plasmid DNA.

Animals. The *Hnf1α* mice used in this study have been generated and characterized previously (29) and were examined at young age (2–4 wk). All procedures were performed in accordance with National Institutes of Health guidelines for the care and use of laboratory animals and with the approval of the Committee for Animal Rights of the UCL Medical School (Brussels, Belgium).

Northern blot and immunoblot analyses. Total RNA was isolated from freshly dissected kidneys of 15- to 18-day-old *Hnf1a* mice by using the guanidium thiocyanate-acid phenol method, separated in a denaturing agarose gel, and transferred on a nylon membrane. The blot was hybridized with a radiolabeled cDNA fragment corresponding to the 1.6-kb sequences of the 3′-end of the *Clcn5* open reading frame (exons 8–12) and then with a β-actin cDNA control probe (Clontech, Mountain View, CA) for normalization. The specificity of the cDNA probe to the *Clcn5* transcript was verified by the absence of its hybridization to the most closely related *Clcn4* transcript. Immunoblotting for ClC-5 was performed as described (43). Briefly, mouse PT cells (mPTC) lysates were separated on nitrocellulose and incubated overnight at 4°C with affinity-purified SB499 antibodies against ClC-5 (43), washed, incubated with peroxidase-labeled antibodies (Dako, Glostrup, Denmark), and visualized with enhanced chemiluminescence. The blots were stripped and reprobed with the anti-β-actin antibody (Sigma, St. Louis, MO) for normalization.

Microdissection of individual nephron segments. Individual nephron segments were microdissected from *Hnf1α* kidneys as described by Terryn et al. (39). Thin coronal slices were prepared from freshly dissected decapsulated kidneys to separate the cortex and medulla at 4°C in HBSS containing glycine, alanine, and D-glucose buffered to pH 7.4 and 325 mosmol/kgH_2O. The cortical and medullary tissue was then digested with collagenase type II (1 mg/ml) for 30 min (for PT) and up to 1 h (other tubules) at 37°C. After digestion, the tubule suspension was washed with albumin (10 mg/ml) and placed on a stage of an inverted microscope. A total of 50 PT (S1 and S2), TAL, and CD segments were collected and placed in 300 μl RLT-buffer (Qiagen, Hilden, Germany) containing 2-mercaptoethanol. Total RNA was extracted immediately after microdissection using an RNeasy Micro Kit (Qiagen) according to the manufacturer's instructions. Quality and concentration of the isolated RNA preparations were analyzed using the 2100 BioAnalyzer (RNA Pico chip from Agilent Technologies, Palo Alto, CA). Total RNA samples were stored at −80°C.

Primary culture of mouse PT cells. Primary cultures of mPTC were prepared from *Hnf1α* mice aged 6 wk, as described previously (39). PT fragments were seeded onto collagen-coated PTFE filter membranes (Transwell-COL, Costar, Corning) in culture medium [DMEM:F12 with 15 mM HEPES, 0.55 mM Na-pyruvate, 0.1 ml/l nonessential amino acids and the SingleQuots Kit (Lonza, Verviers, Belgium) containing hydrocortisone, hEGF, FBS, epinephrine, insulin, triiodothyronine, transferrin, gentamicin/amphotericin, pH set to 7.4 and osmolality at 325 mosmol/kgH_2O] and incubated in a humidified chamber at 37°C-5% CO_2. The medium was replaced every 48 h, and a confluent monolayer of mPTC was expanded from the tubular fragments after 6–7 days.

Plasmids and site-directed mutagenesis and transfection of mPTC. In vitro mutagenesis was carried out on a Rous sarcoma virus (RSV)-driven full-length human HNF1α expression vector (5,981-kb plasmid DNA) (1) using a QuickChange Lightning Site-Directed Mutagenesis Kit (Stratagene, Agilent) following the manufacturer's protocol. The H1 mutant, corresponding to the pathogenic T10M mutation in the dimerization domain of HNF1α (9), was generated by PCR using two oligonucleotide primers, each complementary to opposite strands of the vector: 5′-aaactgagccagctgcagaTggagctcctg-3′ and 5′-caggagctccAtctgcagctggctcagttt-3. The identity of the mutant plasmid was verified by sequencing with a BigDye terminator kit (PerkinElmer Applied Biosystems) and analysis on an ABI3100 capillary sequencer (PerkinElmer Applied Biosystems).

The mPTC were transiently transfected at ~80% confluency by incubation with the plasmid containing either the wild-type or the H1 mutant HNF1α and Fugene HD (Roche): 1 μg plasmid was added to Fugene HD in the culture medium. After 24 h of incubation, cells were harvested for real-time qPCR and immunoblotting. The efficiency of transfection for both plasmids was similar and verified by immunoblotting for the c-myc tag. Total RNA was extracted from mPTC with an RNAqueous kit (Applied Biosystems). For protein extraction, mPTC were washed with PBS, solubilized in ice-cold 10% SDS lysis buffer containing protease inhibitors (Complete Mini; Roche Diagnostics), and centrifuged at 1,000 *g* for 15 min at 4°C. The pellet (nuclear extract) was suspended in ice-cold lysis buffer. Supernatant and pellet were stored at −80°C. Protein concentrations were determined with a bicinchoninic acid protein assay using BSA as standard.

Real-time PCR. Real-time PCR was performed as described previously (16). The reverse transcriptase reaction was performed using an iScript TM cDNA Synthesis Kit (Bio-Rad Laboratories, Hercules, CA). Changes in target gene mRNA levels were determined by relative RT-qPCR with a CFX96 Real-Time PCR Detection System (Bio-Rad) using iQ SYBR Green Supermix (Bio-Rad) to detect single PCR product accumulation. Specific primers were designed using Primer3 (34) (Supplemental Table 2). PCR conditions were 94°C for 3 min followed by 40 cycles of 30 s at 95°C, 30 s at 60°C, and 1 min at 72°C. The PCR products were purified and sequenced using an ABI3100 capillary sequencer (PerkinElmer Applied Biosystems). The efficiency of each set of primers was determined by dilution curves (Supplemental Table 2). The relative changes in target over *GAPDH* mRNAs was calculated using the $2^{-\Delta\Delta}$Ct formula (27). Real-time PCR results were confirmed using two reference genes, *GAPDH* and *HPRT1*. The PCR conditions used to characterize the microdissected nephron segments were: 94°C for 3 min followed by 35 cycles of 30 s at 95°C, 30 s at 60°C, and 1 min at 72°C with FastStart Taq polymerase (Roche, Vilvoorde, Belgium). The PCR products were separated on a 2% agarose gel.

Statistical analysis. All values are expressed as means ± SE. Statistical significance was assessed using a two-tailed Student's *t*-test (GraphPad Software, San Diego, CA).

RESULTS

Distribution of ClC-5 and Hnf1α transcripts during development. Whole mount in situ hybridization showed early expression of *Clcn5* in the somitic lineage (Supplemental Fig. 1a). At *E10.5*, *Clcn5* was readily detected in dermomyotome stripes covering the lateral portion of the somite and in the anlagen of the forelimbs and hindlimbs (Supplemental Fig. 1b). Somitic expression was maintained in the ventrolateral migratory myotomes along the body wall at *E12.5* (Supplemental Fig. 1c). High-resolution hybridization of *E14.5* mouse embryos confirmed *Clcn5* expression in skeletal muscles and, in addition identified strong expression sites in the PT of the developing kidney and in intestinal epithelia, where it overlaps with the expression of *Hnf1*α (Fig. 1, *A* and *B*, adjacent sections). The expression of *Clcn5* in muscle tissue strongly resembles that of *MyoD*, a classic marker for skeletal muscle differentiation (Fig. 1, *B* and *C*). Although *Hnf1*α is also expressed in other tissues like liver and pancreas, our results demonstrate that both *Hnf1*α and *Clcn5* are highly expressed in absorptive epithelia during mouse development, including the yolk sac (data not shown), the primitive gut, and the PT of the kidney.

Transcriptional-regulatory sequences in mouse Clcn5 and human CLCN5 gene loci. In silico analysis of the CLC gene family revealed 11 potential, conserved HNF1 binding consensus sequences in the *Clcn5* locus, three sites for *Clcn3*, one for *Clcn7*, and none for the other isoforms including the kidney-specific *Clcnka* and *Clcnkb* (Supplemental Fig. 2). The pre-

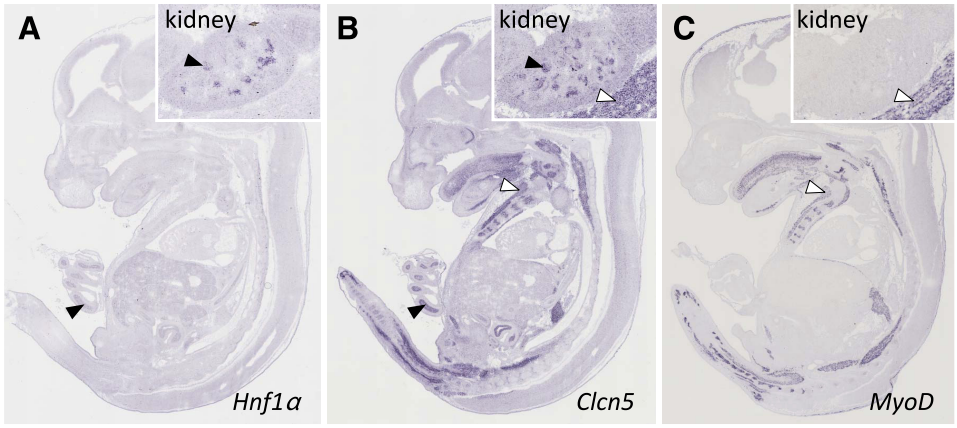

Fig. 1. High-resolution in situ hybridization of hepatocyte nuclear transcription factor (*Hnf1α*), chloride channel 5 (*Clcn5*), and *MyoD* in an embryonic *day 14.5* (*E14.5*) mouse embryo. Sagittal cryosections of whole C57BL/6J mouse embryos were hybridized with antisense digoxygenin-labeled probe derived from corresponding cDNA fragments. *A*: signal for the transcription factor *Hnf1α* is strongest in epithelial structures of the kidney. Moderate signal can be observed in gut epithelia as well as in liver and pancreas (not shown). *B*: high *Clcn5* expression is detected in epithelial structures of the kidney as well as in gut epithelia and all skeletal muscles. *C*: muscle differentiation marker *MyoD* is exclusively expressed in skeletal muscles. *A–C*: *insets* are at a ×4 higher magnification than the embryos. Black arrowheads indicate kidney and gut epithelia. White arrowheads point at skeletal muscles. While in *A* and *B* sections are directly adjacent, *C* depicts a comparable section.

dicted HNF1 binding sites in the 5′-regulatory regions of *Clcn5/CLCN5* and their matching scores to the consensus gGTTAATNaTTaNcN sequence (41) are listed in Fig. 2*A*. The binding site mBS-1 is mouse specific, residing within the enhancer region in the first intron of *Clcn5* (38). In contrast, the hBS-3 contains a canonical consensus (−1056 nt), which appeared to be human specific. The mouse and human 5′-regulatory sequences are well conserved in the first and the second exons, and to a lesser extent in the first intron (Fig. 2*B*). Several nucleotide substitutions and insertion/deletion at the 3′-end of the human alternative exon 1b must have compromised the efficiency of the donor splice site. This may explain the existence of the variant form that includes exon 1b in humans (14) but not in rodents (38). Notably, the six putative HNF1 binding sites in four clusters (BS-1 to BS-4) were all located within conserved sequence segments, implying these regions are likely to contain regulatory functions. Relevance of the in silico prediction was assessed in vitro, with established bandshift patterns (30) observed for putative HNF1 binding sequences in mouse *Clcn5* (at +1931 nt) and in human *CLCN5* (at −1056 nt) (Supplemental Fig. 3). A β-fibrinogen sequence with a known HNF1 binding site was used as a positive control, and for the competition assay. The bandshift assay also confirmed the greater binding affinity of the human sequence at −1056 nt [**, hidden Markov model (HMM) score = 12.4] was demonstrated compared with the mouse sequence at +1931 nt (*, HMM score = 5.4).

In vivo binding of HNF1α to the mouse Clcn5 genomic locus. In vivo binding of HNF1α to the *Clcn5*-regulatory region was further analyzed by ChIP assay on the mouse kidney (Fig. 3). Five of seven binding sites analyzed showed a significant enrichment upon immunoprecipitation with the HNF1α-specific antibody (normalized to a known DNA fragment of *Acta2* devoid of HNF1 binding element), with the maximum at the doublet sites at −4340/−4320 nt upstream of the transcription start site. A number of unbound sites located in other gene loci revealed a mean fold-enrichment of 1.07 ± 0.04, indicating a reliable technique with a baseline close to 1.0 (data not shown).

Luciferase reporter assay of mouse and human ClC-5 promoters. We previously identified promoter and enhancer elements necessary for mouse *Clcn5* transcription (38). In this study, the human orthologous sequences were first isolated from a human X chromosome cosmid library, subcloned into the pXP2 promoterless luciferase vector, and their relative promoter activities were examined in the COS-6 cells (Fig. 4, *A* and *B*). The mouse Mm-pHXh4kb that contains the promoter and enhancer showed a ~1,000-fold relative luciferase activity, whereas a much lower transcriptional activity

A

HNF1 binding consensus
gGTTAATNaTTaNcN

BS no.	Position	Putative binding sequence	HMM SCORE	P-value
mBS-1	+1931	TGTAAATATTTAACT	5.4	0.016
(hBS-1	+1720	TGTAAATCTTAGACT	-0.7	0.22)
mBS-2	+962	GTTTTAAGATTAACT	4.8	0.021
hBS-2	+865	GGTTTAAGATTAACT	7.9	0.0043
mBS-3	-1952	GATTAATGATTACAG	4.8	0.023
hBS-3	-839	GATTAATGAGTACCA	5.9	0.014
(mBS-3	-2169	GGTCAATGTTAAATG	2.4	0.062)
hBS-3	-1056	GGTTAATGTTTAACA	12.4	0.00018
mBS-4	-4320	AGTTACTATTCAGCC	4.4	0.027
hBS-4	-9226	AGTTACTGTTCAGCC	5.8	0.015
mBS-4	-4340	TGTTAGTGTTTAACT	5.2	0.019
hBS-4	-9246	TGTTAGTGTTTAACT	5.2	0.019
mBS-5	-8196	GGTTAATCATATGCC	6.2	0.012
(hBS-5	-12601	AGTTAACCACATGCC	-5.0	0.81)

B

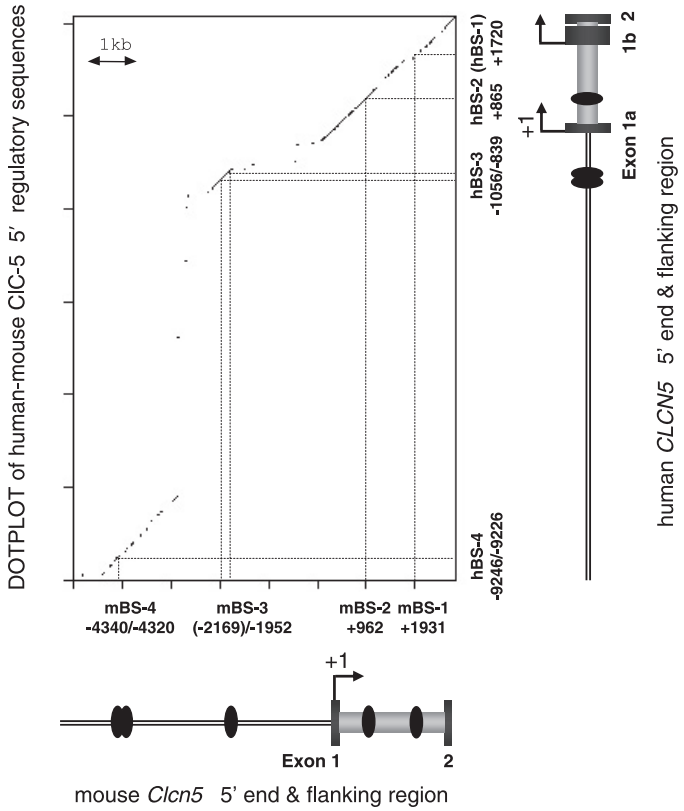

Fig. 2. Comparison of the mouse *Clcn5* and human *CLCN5* regulatory sequences. *A*: conservation of HNF1 binding sequences between mouse and human. Nucleotide positions and their sequences were shown with their calculated scores in fitting to the consensus sequence. HMM, hidden Markov model. *B*: dot plot comparison of the mouse and human 5′-end and upstream sequences (from EMBL accession nos. AL808124 and AL663118, respectively) depicted by using EMBOSS (32). The putative HNF1 binding sites (BS-1–BS-4) are shown as ovals with their nucleotide positions from the annotated transcription start site (+1) (14, 38). The sequence conservation histograms are adopted from the University of California Santa Cruz (UCSC) genome browser (http://genome.ucsc.edu/). Note that mBS-5, which is mouse specific, does not appear in the alignment shown in Fig. 3.

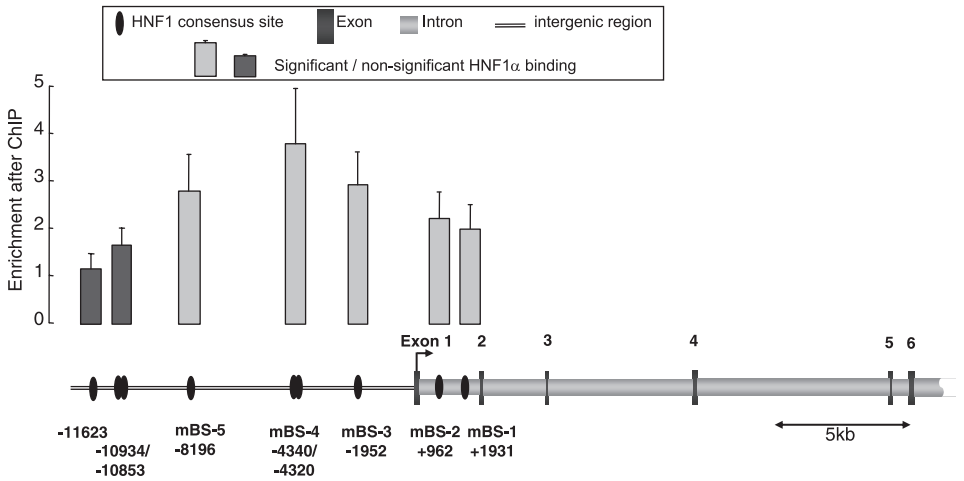

Fig. 3. In vivo binding of HNF1α to its chromatin target sites in the *Clcn5* gene. Putative HNF1 binding sites predicted in silico were subjected to chromatin immunoprecipitation (ChIP) assay. The enrichment for each DNA fragment upon immunoprecipitation of HNF1α is shown in relative to the DNA amplification of an intronic sequence of the aortic smooth muscle α-actin 2 gene, which is devoid of HNF1 binding. Each putative HNF1 binding site is depicted as an oval with its nucleotide position from the transcription start sites.

(~50-fold) was observed for the human orthologous construct Hs-pBmXh5kb.

To examine the effect of HNF1α on the transcriptional activities in vitro, each construct was cotransfected either with a control vector pGEM or with a vector expressing human HNF1α in the C33 cells which lack endogenous HNF1α expression (Fig. 4, *C–F*). The mouse construct pMm-F3Xh2kb and the human construct pHs-BgXh2kb, which harbor HNF1 binding loci BS-1 and/or BS-2, displayed similar basal luciferase activities. While the mouse construct was strongly activated by HNF1α coexpression, the human construct without binding consensus at BS-1 did not respond significantly (Fig. 4*C*). When the further upstream sequences with doublets of binding sites hBS-3 were included in the human construct Hs-pBmXh5kb, HNF1α transactivated its activity by twofold (Fig. 4*D*). Mouse constructs Mm-pHXh4kb and Mm-pBmB5kb, embracing mBS-1 and -2 and mBS-3 and -4, respectively, were both transactivated by HNF1α (Fig. 4, *E* and *F*). In contrast, the minimal promoter construct Mm-pBgB1.3kb, which lacks mBS-3 and -4, was nonresponsive to HNF1α (Fig. 4*F*). The results demonstrated the functional relevance of the multiple HNF1 binding sites to both mouse and human *Clcn5/CLCN5* gene loci, with species-dependent variation in the contribution of each site.

Hnf1α regulates expression of ClC-5 in proximal tubules in vivo. To verify that the *Clcn5* gene is regulated by HNF1α in vivo, we measured its expression at the mRNA and protein levels in kidneys from *Hnf1α*-null mice (Fig. 5). The deletion of HNF1α was reflected by a significant decrease in *Clcn5* mRNA (Fig. 5*A*) and ClC-5 protein (Fig. 5*B*) compared with wild-type *Hnf1α* controls. To further address the segment-specific regulation of ClC-5, and the role of HNF1α vs. HNF1β, which is also expressed in the distal nephron, we used microdissected segments obtained from *Hnf1α* kidneys (Fig. 5. *C* and *D*). Enrichment in specific markers validated the samples obtained from the proximal (AQP1) and more distal (NKCC2, AQP2) nephron segments (Fig. 5*C*; Supplemental Table 3). Quantitative analysis (qPCR) revealed that the deletion of HNF1α in PT segments was reflected by an ~60% decrease in *Clcn5* mRNA expression, despite a significant upregulation of *Hnf1β* in these samples. In contrast, *Hnf1α* was much less abundant in distal segments, which dominantly expressed *Hnf1β*, and its deletion was not associated with a decrease in *Clcn5* mRNA expression (Fig. 5*D*).

Regulation of ClC-5 expression in mPTC derived from Hnf1α kidneys. The direct effect of HNF1α on the expression of ClC-5 was analyzed in mPTC obtained from *Hnf1α* kidneys (Fig. 6). The expression of ClC-5 mRNA (Fig. 6*A*) and protein (Fig. 6*B*) was significantly reduced in mPTC from $Hnf1\alpha^{-/-}$ compared with mPTC from $Hnf1\alpha^{+/+}$ kidneys. The transfection of $Hnf1\alpha^{-/-}$ mPTC with wild-type HNF1α rescued the expression of ClC-5 to a normal level, whereas transfection with mock or mutant HNF1α had no significant effect. Of note, the rescue of ClC-5 expression in mPTC was paralleled by that of SGLT2, whereas the expression of SGLT1, which is not regulated by HNF1α in the mouse (29), was unchanged (data not shown).

DISCUSSION

In this study, we show that the transcription factor HNF1α positively regulates the expression of ClC-5 in the PT of the kidney. In silico prediction identified a number of conserved HNF1 binding sites within the 5′-regulatory regions of the *CLCN5/Clcn5* genes, whose binding and transcriptional activities were confirmed in vivo and in vitro. Furthermore, we showed that the direct transcriptional regulation of ClC-5 by HNF1α was specific to the PT segment. Taken together, these data indicate that HNF1α is an essential regulator of the tissue-specific expression of the endosomal Cl^-/H^+ exchanger ClC-5 in absorptive epithelia. These results emphasize the role of HNF1α in the differentiation of the PT and the potential for renal manifestations associated with mutations of HNF1α in MODY3 patients.

The enrichment of HNF1 binding consensus sites in the ClC-5 gene locus stands among the mammalian CLC gene family, with no putative site identified in the loci of ClC-Ka and ClC-Kb, which are selectively expressed in distal nephron segments but not in the PT (15). ClC-4, which shares at least 80% sequence identity with ClC-5, does not contain any putative HNF1 binding sites but instead has GC-rich sequences characteristic of housekeeping genes (data not shown). These data suggest that tissue-specific transcriptional regulation sustains the specific roles played by members of the CLC gene family in higher organisms.

We demonstrate the tissue-specific distribution of ClC-5 during mouse development and nephrogenesis. In particular, ClC-5 is predominantly expressed in polarized absorptive epithelia such as the primitive gut, the mesonephric bud, and the extraembryonic yolk sac, which contains an extensive vesicular system similar to the structure of the renal PT (22). In the yolk sac, the expression of *Clcn5* spatially and temporarily overlaps with that of *Hnf1α* (2), whereas there is a striking

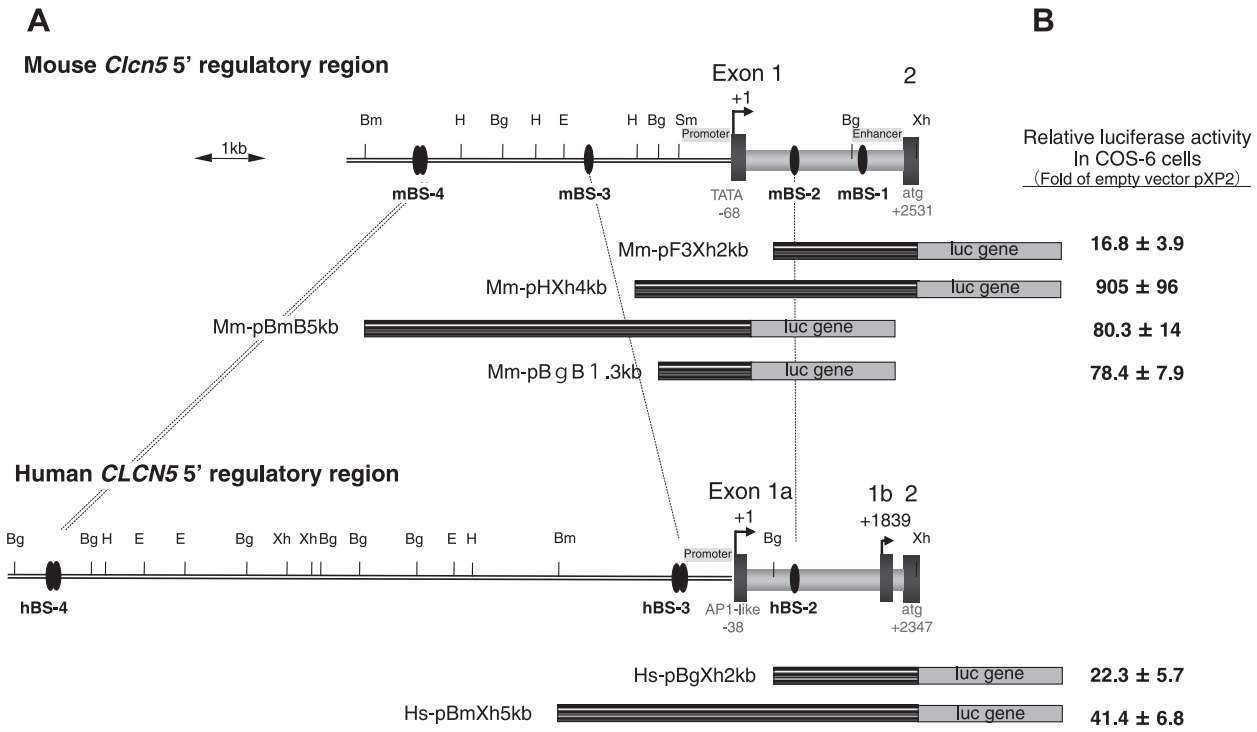

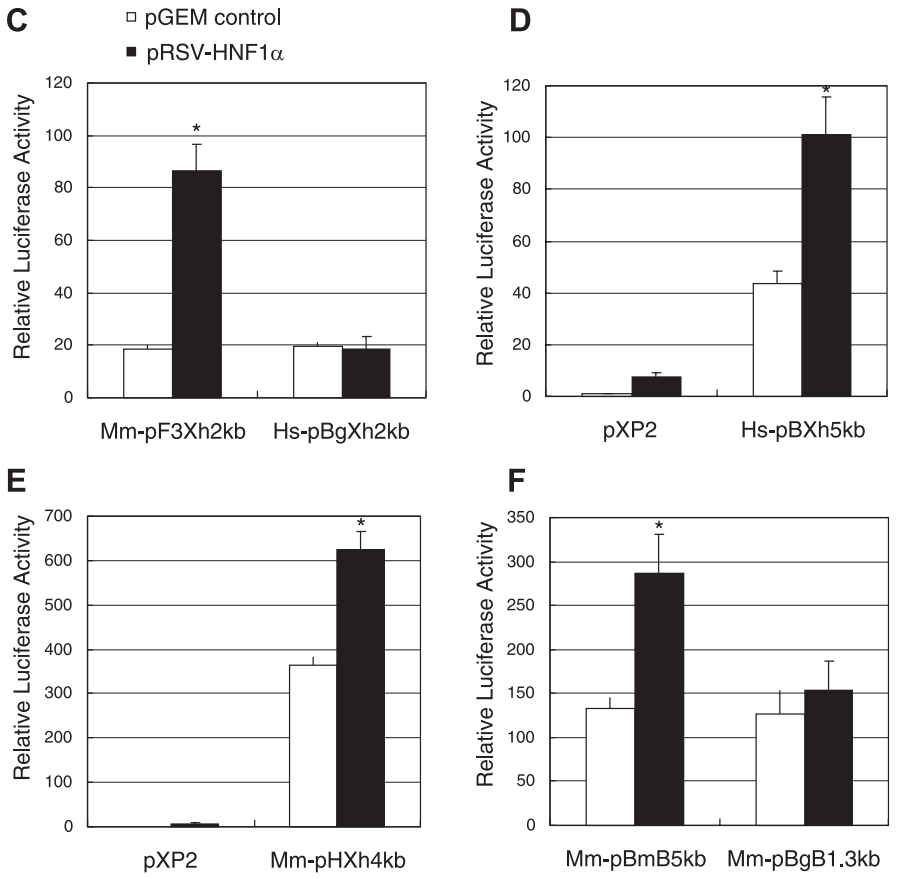

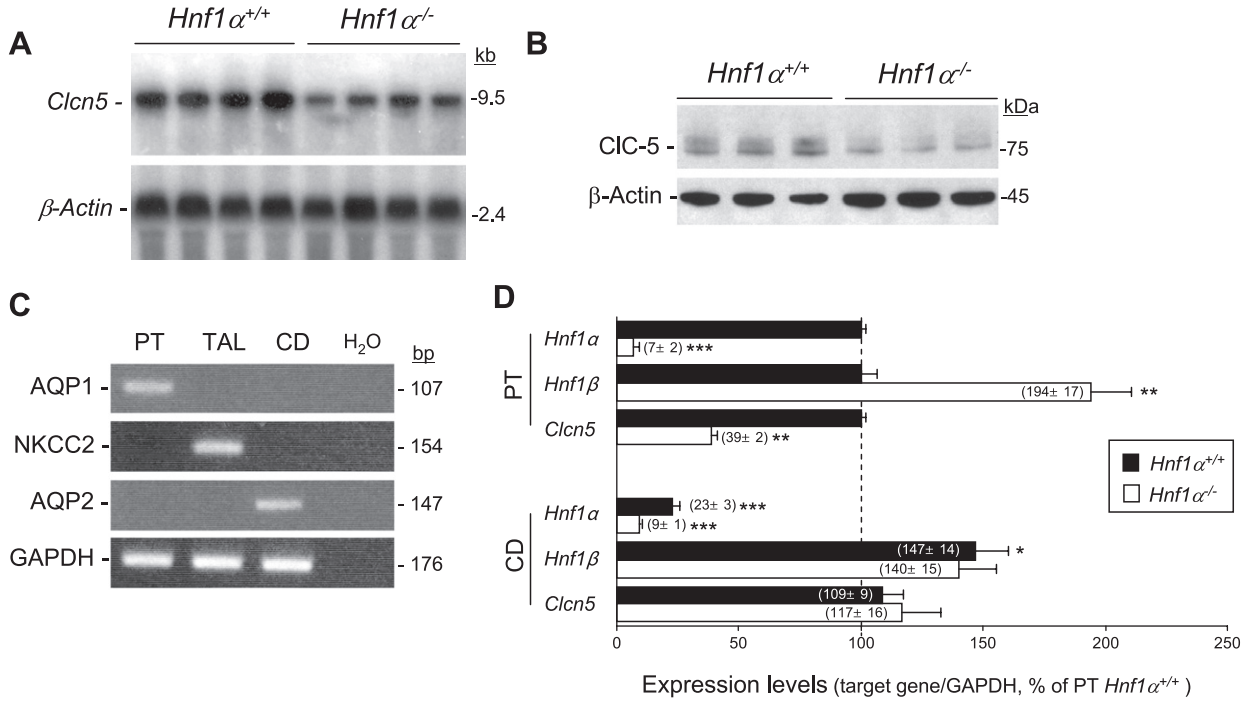

Fig. 5. Renal and segmental expression of *Clcn5* mRNA and ClC-5 in *Hnf1α* mice. *A*: Northern blot analysis for *Clcn5* and *β-actin* on total RNA (15 μg/lane) from kidneys of 4 pairs of *Hnf1α* mice. *B*: immunoblotting for ClC-5 and β-actin in kidney extracts from 3 pairs of *Hnf1α* mice. *C* and *D*: expression of *Hnf1α*, *Hnf1β*, and *ClCn5* mRNA in microdissected segments of *Hnf1α* kidneys. *C*: enrichment of specific markers by semiquantitative RT-PCR in proximal tubule [PT; aquaporin-1 (AQP1)], thick ascending limb [TAL; Na-K-2Cl cotransporter (NKCC2)], and collecting duct (CD; AQP2) samples. *D*: relative expression of *Hnf1α*, *HNF1β*, and *Clcn5* mRNA by qPCR in PT and CD segments, with the expression of each transcript in *Hnf1α*$^{+/+}$ PT taken as 100% ($n = 4$ samples from 4 pairs of mice). *$P < 0.05$, **$P < 0.01$, ***$P < 0.001$ vs. PT *Hnf1α*$^{+/+}$ level.

overlap between the expression of the two genes in kidney and intestine epithelia at *E14.5*. In the earlier stage, HNF1α expression is shown to start only from *E10.5* in the developing liver primordium, intestine, and mesonephros (29). By contrast, abundant expression of HNF1β precedes that of HNF1α in these organs (3) and therefore correlates better with the observed ClC-5 expression at *E9–10*. Accordingly, HNF1β may initiate ClC-5 expression during early organogenesis, and HNF1α may reinforce its predominant expression in absorptive tissues, and particularly in PT cells, at later stages of differentiation (17). The specific expression of ClC-5 in the myogenic lineage contrasted with its reputation of a gene predominantly expressed in the kidney and the lack of apparent muscular manifestations in patients with Dent's disease or ClC-5 KO mice. Both ClC-4 and ClC-5 function as Cl^-/H^+ exchangers (35), and ClC-5 may share a redundant role with ClC-4, whose expression is predominant in skeletal muscles (15).

By ChIP analysis, we confirmed the binding of HNF1α to the 5′-regulatory regions of the *Clcn5* gene in mouse kidney. The ClC-5 mRNA and protein expression was reduced in the PT segments and mPTC of HNF1α-null mice. Inversely, normal expression levels were obtained upon transfection of the HNF1α-null mPTC with wild-type HNF1α. Of note, the expression of HNF1β was increased by about twofold in the HNF1α-null PT segments, suggesting a compensation for the loss of HNF1α. However, this was insufficient to maintain the full expression of ClC-5, at least in the time point investigated. The fact that ClC-5 expression in the PT is regulated, at least in part, by HNF1α may have clinical consequences. Autosomal dominant mutations in the human gene (*HNF1A* or *TCF1*) coding for HNF1α cause a particular form of diabetes called maturity onset diabetes of the young type 3 (MODY3) (9). The disease, which is associated with a defect in insulin secretion that appears frequently in young patients, is characterized by a highly variable phenotype. Of interest, a slight degree of low-molecular-weight proteinuria is detected in a subset of patients harboring mutations in HNF1α and in Hnf1α KO mice (data not shown). The latter observation is consistent with the low-molecular-weight proteinuria detected in heterozygous carriers of mutations in ClC-5 (36, 43). By

Fig. 4. Anatomy and activity of the mouse and human ClC-5 gene promoters. *A*: schematic representation of the 5′ control regions. Each putative HNF1 binding site is depicted as an oval with its nucleotide position from the transcription start sites. The conserved orthologous binding loci BS-2 to BS-4 are indicated with dotted lines between mouse and human. Restriction sites are *Bam*HI (B), *Bgl*II (Bg), *Eco*RI (E), *Hin*dIII (H), and *Xho*I (Xh). *B*: transcriptional activities of genomic sequences of the ClC-5 promoters were measured in COS-6 cells and compared with promoterless luciferase reporter vector pXP2. Each measure is the average of 3–9 independent transfections. *C–F*: HNF1α-dependent transactivation of the ClC-5 gene promoter-luciferase constructs. The constructs shown in *A* were cotransfected into the C33 cells with either an HNF1α-expressing vector or pGEM plasmid DNA as a negative control. Values represent relative luciferase activity over the promoterless pXP2 vector cotransfected with pGEM plasmid DNA. Each measure is the average of 3–9 independent transfections. *$P < 0.05$ vs. control.

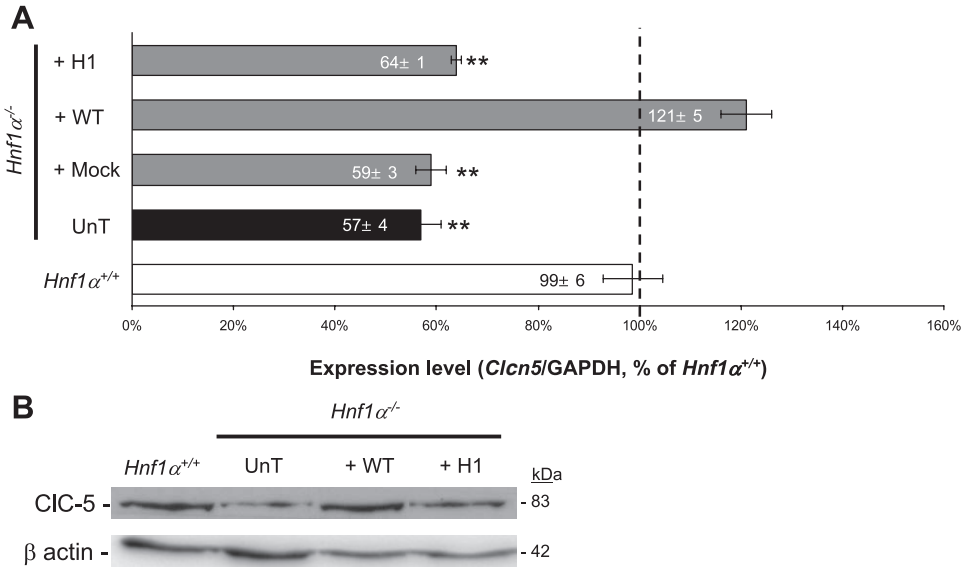

Fig. 6. Expression of ClC-5 in mouse PT cells derived from *Hnf1α* mice. *A*: mRNA expression of *Clcn5* was analyzed by real-time PCR in mouse PT cells derived from $Hnf1\alpha^{+/+}$ (open bar) or $Hnf1\alpha^{-/-}$ (black and grey bars) kidneys. Compared with wild-type $Hnf1\alpha^{+/+}$ mouse PT cells, the expression of *Clcn5* was significantly reduced in untransfected $Hnf1\alpha^{-/-}$ cells (UnT; black bar). Transfection of $Hnf1\alpha^{-/-}$ mouse PT cells with wild-type HNF1α (+ WT) induced the expression of *Clcn5* to a level similar to that in $Hnf1\alpha^{+/+}$, whereas transfection with mock or H1 mutant HNF1α (+H1) had no effect (grey bars). Values are means ± SE of 5 individual experiments. $^{**}P < 0.01$ vs. $Hnf1\alpha^{+/+}$ mouse PT cells. *B*: representative immunoblotting of ClC-5 in lysates from mouse PT cells obtained from *Hnf1α* kidneys. Protein levels of ClC-5 are reduced in untransfected $Hnf1\alpha^{-/-}$ mPTC (UnT), whereas transfection of wild-type (+ WT) but not that of mutant (+ H1) HNF1α induced the expression of ClC-5.

extension, one could hypothesize that variants in *TCF1* may modulate the phenotype of Dent's disease.

Thus far, there is no evidence that HNF1α and HNF1β bind to different sequences, and a previous ChIP analysis of the mouse kidney revealed in vivo binding of both factors to every HNF1 binding site examined (11). Consistent with this, we observed that not only HNF1α but also HNF1β binds to the *CLCN5/Clcn5* gene promoters and that their coexpressions enhance their promoter activities in vitro (data not shown). In the kidney, HNF1α is specifically expressed in PT segments whereas HNF1β is expressed in all tubular segments and CD (11, 29). Accordingly, the ClC-5 expression in the TAL and CD could be under the regulation of HNF1β rather than HNF1α, as supported by our segment-specific expression data (Fig. 5*D*). The renal-restricted inactivation (mainly in the TAL and CD) of HNF1β in mice resulted in renal cyst formation due to defective transcriptional activation of genes localized in the primary cilium of epithelial cells, whose mutations are individually responsible for cystic kidney diseases (11). Notably, small cysts are commonly observed in the cortex and medulla of the kidneys of patient with Dent's disease (44). It is tempting to speculate that ClC-5 is another target of HNF1β in distal nephron segments, where ClC-5 may regulate the active trafficking of stereocilia membrane proteins. The expression of ClC-5 in the α-type intercalated cells could also be regulated by specific transcription factors involved in the maturation of these cells, including the forkhead transcription factor Foxi1 (16, 24).

Comparative analysis of the *CLCN5/Clcn5* promoters revealed that transcriptional activities of the mouse 5′ sequences are strikingly more potent than that of human. The difference may arise from the fact that the mouse first intron sequence harbors effective enhancer elements (38), whereas the human sequence contains suppressor elements (14). The mouse HNF1 binding consensus at +1931 within this enhancer region is lost in the human orthologous locus, and the transcriptional response to HNF1α coexpression is abolished. Instead, a specific HNF1 binding site with strongest binding affinity is found in the human 5′ sequences. Conserved biological functions are under the control of evolutionarily preserved regulatory mechanisms in many cases, although evolution may also create novel configurations by deletions or insertions of relatively large fragment of genomic DNA. This must have been the case with ClC-5, where mouse and human genomic structures have been remodeled: the binding manner of HNF1α is known to be variable between these species, despite the highly conserved function of the transcription factor (25). Nevertheless, given the relatively large number of HNF1 binding sites that we could identify in both the human and mouse, it is difficult to imagine that the loss of a single site would have a dramatic consequence on the control of gene expression.

In conclusion, the present study established that HNF1α positively regulates the transcription of ClC-5 in the PT, and its contribution is conserved between mouse and human with some species diversity. Our data also demonstrate a wider functional distribution of ClC-5 during development than was anticipated from the phenotype of human patients with Dent's disease and its mouse models. These data give insights into the mechanisms governing epithelial differentiation, in parallel to other transcription factors (e.g., ZONAB) that are associated with epithelial cell proliferation during development (19).

ACKNOWLEDGMENTS

We thank Dr. C. Cheret, A. Doyan, Dr. Y. Ninomiya, Dr. A. Reimann, and H. Debaix for help and advice on transfection, ChIP analysis protocols, and expression studies.

GRANTS

K. Tanaka was supported by the UK National Kidney Research Fund. O. Devuyst was financially supported by the Belgian agencies Fonds de la Recherche Scientifique and Fonds de la Recherche Scientifique Médicale, the "Fondation Alphonse & Jean Forton," a Concerted Research Action (05/10-328), an Inter-university Attraction Pole (IUAP P6/05), the DIANE project (Communauté Française de Belgique), and the EUNEFRON (FP7, GA 201590) program of the European Community. M. Pontoglio was financially supported by the Fondation pour la Recherche Médicale and the Fondation Bettencourt-Schueller (Prix Coup d'Elan).

DISCLOSURES

No conflicts of interest, financial or otherwise, are declared by the authors.

REFERENCES

1. **Bach I, Yaniv M.** More potent transcriptional activators or a transdominant inhibitor of the HNF1 homeoprotein family are generated by alternative RNA processing. *EMBO J* 12: 4229–4242, 1993.
2. **Blumenfeld M, Maury M, Chouard T, Yaniv M, Condamine H.** Hepatic nuclear factor 1 (HNF1) shows a wider distribution than products of its known target genes in developing mouse. *Development* 113: 589–599, 1991.
3. **Cereghini S, Ott MO, Power S, Maury M.** Expression patterns of vHNF1 and HNF1 homeoproteins in early postimplantation embryos suggest distinct and sequential developmental roles. *Development* 116: 783–797, 1992.
4. **Cheret C, Doyen A, Yaniv M, Pontoglio M.** Hepatocyte nuclear factor 1 alpha controls renal expression of the Npt1-Npt4 anionic transporter locus. *J Mol Biol* 322: 929–941, 2002.
5. **Christensen EI, Verroust PJ, Nielsen R.** Receptor-mediated endocytosis in renal proximal tubule. *Pflügers Arch* 458: 1039–1048, 2009.
6. **D'Angelo A, Bluteau O, Garcia-Gonzalez MA, Gresh L, Doyen A, Garbay S, Robine S, Pontoglio M.** Hepatocyte nuclear factor 1alpha and beta control terminal differentiation and cell fate commitment in the gut epithelium. *Development* 137: 1573–1582, 2010.
7. **Devuyst O, Christie PT, Courtoy PJ, Beauwens R, Thakker RV.** Intra-renal and subcellular distribution of the human chloride channel, CLC-5, reveals a pathophysiological basis for Dent's disease. *Hum Mol Genet* 8: 247–257, 1999.
8. **Devuyst O, Guggino WB.** Chloride channels in the kidney: lessons learned from knockout animals. *Am J Physiol Renal Physiol* 283: F1176–F1191, 2002.
9. **Ellard S, Colclough K.** Mutations in the genes encoding the transcription factors hepatocyte nuclear factor 1 alpha (HNF1A) and 4 alpha (HNF4A) in maturity-onset diabetes of the young. *Hum Mutat* 27: 854–869, 2006.
10. **Gorski K, Carneiro M, Schibler U.** Tissue-specific in vitro transcription from the mouse albumin promoter. *Cell* 47: 767–776, 1986.
11. **Gresh L, Fischer E, Reimann A, Tanguy M, Garbay S, Shao X, Hiesberger T, Fiette L, Igarashi P, Yaniv M, Pontoglio M.** A transcriptional network in polycystic kidney disease. *EMBO J* 23: 1657–1668, 2004.
12. **Günther W, Lüchow A, Cluzeaud F, Vandewalle A, Jentsch TJ.** ClC-5, the chloride channel mutated in Dent's disease, colocalizes with the proton pump in endocytotically active kidney cells. *Proc Natl Acad Sci USA* 95: 8075–8080, 1998.
13. **Günther W, Piwon N, Jentsch TJ.** The ClC-5 chloride channel knockout mouse—an animal model for Dent's disease. *Pflügers Arch* 445: 456–62, 2003.
14. **Hayama A, Uchida S, Sasaki S, Marumo F.** Isolation and characterization of the human CLC-5 chloride channel gene promoter. *Gene* 261: 355–364, 2000.
15. **Jentsch TJ.** CLC chloride channels and transporters: from genes to protein structure, pathology and physiology. *Crit Rev Biochem Mol Biol* 43: 3–36, 2008.
16. **Jouret F, Auzanneau C, Debaix H, Wada GH, Pretto C, Marbaix E, Karet FE, Courtoy PJ, Devuyst O.** Ubiquitous and kidney-specific subunits of the vacuolar H^+-ATPase are differentially expressed during nephrogenesis. *J Am Soc Nephrol* 16: 3235–3246, 2005.
17. **Jouret F, Igarashi T, Gofflot F, Wilson PD, Karet FE, Thakker RV, Devuyst O.** Comparative ontogeny, processing, and segmental distribution of the renal chloride channel, ClC-5. *Kidney Int* 65: 198–208, 2004.
18. **Lazzaro D, De Simone V, De Magistris L, Lehtonen E, Cortese R.** LFB1 and LFB3 homeoproteins are sequentially expressed during kidney development. *Development* 114: 469–479, 1992.
19. **Lima WR, Parreira KS, Devuyst O, Caplanusi A, N'kuli F, Marien B, Van Der Smissen P, Alves PM, Verroust P, Christensen EI, Terzi F, Matter K, Balda MS, Pierreux CE, Courtoy PJ.** ZONAB promotes proliferation and represses differentiation of proximal tubule epithelial cells. *J Am Soc Nephrol* 21: 478–488, 2010.
20. **Lloyd SE, Pearce SH, Fisher SE, Steinmeyer K, Schwappach B, Scheinman SJ, Harding B, Bolino A, Devoto M, Goodyer P, Rigden SP, Wrong O, Jentsch TJ, Craig IW, Thakker RV.** A common molecular basis for three inherited kidney stone diseases. *Nature* 379: 445–449, 1996.
21. **Maizel JV, Lenk RP.** Enhanced graphic matrix analysis of nucleic acid and protein sequences. *Proc Natl Acad Sci USA* 78: 7665, 1981.
22. **Maunoury R, Robine S, Pringault E, Léonard N, Gaillard JA, Louvard D.** Developmental regulation of villin gene expression in the epithelial cell lineages of mouse digestive and urogenital tracts. *Development* 115: 717–728, 1992.
23. **Mellman I, Fuchs R, Helenius A.** Acidification of the endocytic and exocytic pathways. *Annu Rev Biochem* 55: 663–700, 1986.
24. **Moulin P, Igarashi T, Van der Smissen P, Cosyns JP, Verroust P, Thakker RV, Scheinman SJ, Courtoy PJ, Devuyst O.** Altered polarity and expression of H^+-ATPase without ultrastructural changes in kidneys of Dent's disease patients. *Kidney Int* 63: 1285–1295, 2003.
25. **Odom DT, Dowell RD, Jacobsen ES, Gordon W, Danford TW, MacIsaac KD, Rolfe PA, Conboy CM, Gifford DK, Fraenkel E.** Tissue-specific transcriptional regulation has diverged significantly between human and mouse. *Nat Genet* 39: 730–732, 2007.
26. **Parreira KS, Debaix H, Cnops Y, Geffers L, Devuyst O.** Expression patterns of the aquaporin gene family during renal development: influence of genetic variability. *Pflügers Arch* 458: 745–759, 2009.
27. **Pfaffl MW.** A new mathematical model for relative quantification in real-time RT-PCR. *Nucleic Acids Res* 29: e45, 2001.
28. **Piwon N, Günther W, Schwake M, Bösl MR, Jentsch TJ.** ClC-5 Cl^--channel disruption impairs endocytosis in a mouse model for Dent's disease. *Nature* 408: 369–373, 2000.
29. **Pontoglio M, Barra J, Hadchouel M, Doyen A, Kress C, Bach JP, Babinet C, Yaniv M.** Hepatocyte nuclear factor 1 inactivation results in hepatic dysfunction, phenylketonuria, and renal Fanconi syndrome. *Cell* 84: 575–585, 1996.
30. **Pontoglio M, Faust DM, Doyen A, Yaniv M, Weiss MC.** Hepatocyte nuclear factor 1alpha gene inactivation impairs chromatin remodeling and demethylation of the phenylalanine hydroxylase gene. *Mol Cell Biol* 17: 4948–4956, 1997.
31. **Pontoglio M, Prié D, Cheret C, Doyen A, Leroy C, Froguel P, Velho G, Yaniv M, Friedlander G.** HNF1alpha controls renal glucose reabsorption in mouse and man. *EMBO Rep* 1: 359–365, 2000.
32. **Rice P, Longden I, Bleasby A.** EMBOSS: the European Molecular Biology Open Software Suite. *Trends Genet* 16: 276–277, 2000.
33. **Rosen B, Beddington R.** Detection of mRNA in whole mounts of mouse embryos using digoxigenin riboprobes. *Methods Mol Biol* 28: 201–208, 1994.
34. **Rozen S, Skaletsky H.** Primer3 on the WWW for general users and for biologist programmers. *Methods Mol Biol* 132: 365–386, 2000.
35. **Scheel O, Zdebik AA, Lourdel S, Jentsch TJ.** Voltage-dependent electrogenic chloride/proton exchange by endosomal CLC proteins. *Nature* 436: 424–427, 2005.
36. **Scheinman SJ.** X-linked hypercalciuric nephrolithiasis: clinical syndromes and chloride channel mutations. *Kidney Int* 53: 3–17, 1998.
37. **Shih DQ, Bussen M, Sehayek E, Ananthanarayanan M, Shneider BL, Suchy FJ, Shefer S, Bollileni JS, Gonzalez FJ, Breslow JL, Stoffel M.** Hepatocyte nuclear factor-1alpha is an essential regulator of bile acid and plasma cholesterol metabolism. *Nat Genet* 27: 375–382, 2001.
38. **Tanaka K, Fisher SE, Craig IW.** Characterization of novel promoter and enhancer elements of the mouse homologue of the Dent disease gene, CLCN5, implicated in X-linked hereditary nephrolithiasis. *Genomics* 58: 281–292, 1999.
39. **Terryn S, Jouret F, Vandenabeele F, Smolders I, Moreels M, Devuyst O, Steels P, Van Kerkhove E.** A primary culture of mouse proximal tubular cells, established on collagen-coated membranes. *Am J Physiol Renal Physiol* 293: F476–F485, 2007.
40. **Tronche F, Ringeisen F, Blumenfeld M, Yaniv M, Pontoglio M.** Analysis of the distribution of binding sites for a tissue-specific transcription factor in the vertebrate genome. *J Mol Biol* 266: 231–245, 1997.
41. **Tronche F, Yaniv M.** HNF1, a homeoprotein member of the hepatic transcription regulatory network. *Bioessays* 14: 579–587, 1992.
42. **Vandewalle A, Cluzeaud F, Peng KC, Bens M, Lüchow A, Günther W, Jentsch TJ.** Tissue distribution and subcellular localization of the ClC-5 chloride channel in rat intestinal cells. *Am J Physiol Cell Physiol* 280: C373–C381, 2001.
43. **Wang SS, Devuyst O, Courtoy PJ, Wang XT, Wang H, Wang Y, Thakker RV, Guggino S, Guggino WB.** Mice lacking renal chloride channel, CLC-5, are a model for Dent's disease, a nephrolithiasis disorder associated with defective receptor-mediated endocytosis. *Hum Mol Genet* 9: 2937–2945, 2000.
44. **Wrong OM, Norden AG, Feest TG.** Dent's disease; a familial proximal renal tubular syndrome with low-molecular-weight proteinuria, hypercalciuria, nephrocalcinosis, metabolic bone disease, progressive renal failure and a marked male predominance. *Q J M* 87: 473–493, 1994.